

Original Article

High expression of VTA1 is an adverse prognostic factor in lung adenocarcinoma

Xingang Sun¹, Ruixin Wu^{2,*}, Xinjun Guan^{1,*}, Changsheng Dong^{3,4}, Dongze Qiu⁵, Guojie Xia¹, Shouhan Feng¹, Jinlong Duan¹, Lei Zhang⁶

¹ Department of Oncology, Huzhou Hospital of Traditional Chinese Medicine, Zhejiang University of Traditional Chinese Medicine, Huzhou 313000, China

² Preclinical Department, Shanghai Municipal Hospital of Traditional Chinese Medicine, Shanghai University of Traditional Chinese Medicine, Shanghai 200071, China

³ Cancer Institute, Longhua Hospital, Shanghai University of Traditional Chinese Medicine

⁴ Department of Oncology, Longhua Hospital, Shanghai University of Traditional Chinese Medicine, Shanghai 200032, China

⁵ Department of Integrative Medicine, Shanghai Geriatric Medical Center, Shanghai 201104, China

⁶ Department of Acupuncture and Moxibustion Massage Rehabilitation, Huzhou Hospital of Traditional Chinese Medicine, Zhejiang University of Traditional Chinese Medicine, Huzhou 313000, China

Article Info

Abstract



Article history:

Received: November 13, 2023

Accepted: January 17, 2024

Published: January 31, 2024

Use your device to scan and read the article online



Lung adenocarcinoma (LUAD) is a common pathological type of non-small cell lung cancer; identifying preferable biomarkers has become one of the current challenges. Given that VTA1 has been reported associated with tumor progression in various human solid cancers but rarely reported in LUAD, herein, RNA sequencing data from TCGA and GTEx were obtained for analysis of VTA1 expression and differentially expressed gene (DEG). Furthermore, functional enrichment analysis of VTA1-related DEGs was performed by GO/KEGG, GSEA, immune cell infiltration analysis, and protein-protein interaction (PPI) network. In addition, the clinical significance of VTA1 in LUAD was figured out by Kaplan-Meier Cox regression and prognostic nomogram model. R package was used to analyze incorporated studies. As a result, VTA1 was highly expressed in various malignancies, including LUAD, compared with normal samples. Moreover, high expression of VTA1 was associated with poor prognosis in 533 LUAD samples, as well as T stage T2&T3&T4, N stage N1&N2&N3, M stage M1, pathologic stage II&III&IV, and residual tumor R1&R2, et al. ($P < 0.05$). High VTA1 was an independent prognostic factor in Cox regression analysis; Age and cytogenetics risk were included in the nomogram prognostic model. Furthermore, a total of 4232 DEGs were identified between the high- and the low-expression group, of which 736 genes were up-regulated and 3496 genes were down-regulated. Collectively, high expression of VTA1 is a potential biomarker for adverse outcomes in LUAD. The DEGs and pathways recognized in the study provide a preliminary grasp of the underlying molecular mechanisms of LUAD carcinogenesis and progression.

Keywords: Lung adenocarcinoma, Survival, VTA1, Prognostic factor.

1. Introduction

Lung adenocarcinoma (LUAD) is an aggressive malignant tumor characterized by high heterogeneity, variable prognosis, and high mortality. Cytogenetic and molecular abnormalities are presently the main variables in risk assessment and treatment choices. The underlying concrete molecular processes [1, 2]. However, are still not completely understood. Individualized care for LUAD patients has been made possible by the introduction of numerous targeted medicines, improving complete remission (CR) rates and extending life. Unfortunately, the effectiveness of the currently available targeted medication monotherapy or combination therapy with conventional chemotherapy has not yet been as hoped [3]. Therefore, identifying new biomarkers may help us better understand the molecular basis of LUAD, which may be crucial for LUAD dia-

gnosis, prognosis classification, monitoring of carcinoma residuals, therapy response prediction, and perhaps even the creation of targeted drugs.

VTA1 (Vesicle Trafficking 1) is a Protein Coding gene. Diseases associated with VTA1 include Arthrogyriposis, Distal, Type 1B and Arthrogyriposis, Distal, Type 1A [4]. Among its related pathways are HIV Life Cycle and Vesicle-mediated transport. VTA1 has been reported associated with tumor progression in human solid [5]. VTA1 is involved in activities of the multivesicular body, an endosomal compartment involved in sorting membrane proteins for degradation in lysosomes [6]. VTA1 is thought to be a cofactor of VPS4A/B. VTA1 is involved in HIV-1 budding. It has been shown by similarity to be involved in the sorting and down-regulation of EGFR [7]. VTA1 is involved in the endosomal multivesicular bodies (MVB)

* Corresponding author.

E-mail address: wu2004251244@163.com; duijuliang57@163.com (Ruixin Wu, Xinjun Guan).

Doi: <http://dx.doi.org/10.14715/cmb/2024.70.1.7>

pathway. MVBs contain intraluminal vesicles (ILVs) that are generated by invagination and scission from the limiting membrane of the endosome and mostly are delivered to lysosomes enabling degradation of membrane proteins, such as stimulated growth factor receptors, lysosomal enzymes and lipids [8]. VTA1 is thought to be a cofactor of VPS4A/B, which catalyzes and disassembles membrane-associated ESCRT-III assemblies. VTA1 is also involved in the sorting and down-regulation of EGFR (by similarity) [9]. However, to date, the expression of VTA1 in LUAD and its prognostic value remain unclear.

Therefore, in this study, we aimed to ascertain the relationship between the expression level of VTA1 and the prognosis of LUAD by the following three steps: First of all, RNA sequencing (RNA-seq) data of AML samples from the cancer genome atlas (TCGA) and Genotype-Tissue Expression (GTEx) were acquired to analyze the expression of the core gene VTA1. Subsequently, functional enrichment analysis of VTA1 was done via GO, KEGG, GSEA, immune cell infiltration analysis, and protein-protein interaction (PPI) network. Besides, the clinical significance of VTA1 in LUAD was analyzed by Kaplan-Meier and Cox regression and nomogram prognostic model.

In this way, significantly altered genes and pathways would be screened out through gene enrichment analysis and subpathway enrichment analysis, the connection of which with VTA1 may play pivotal role in the occurrence of LUAD.

2. Materials and methods

2.1. RNA-sequencing data and bioinformatics analysis

The pan-cancer RNA-seq data of TCGA and GTEx with toil processed uniformly were downloaded from UCSC XENA (<https://xenabrowser.net/datapages/>) [10-13]. Level 3 HTSeq-FPKM and HTSeq-Count data of the LUAD samples were obtained from the TCGA website (<https://portal.gdc.cancer.gov/repository>) for further analysis. This study was in full compliance with the published guidelines of TCGA and GTEx.

2.2. Differentially expressed gene (DEG) analysis

The DESeq2 R package was adopted to compare expression data of low- and high-expression of VTA1 (cut-off value of 50%) in AML samples (HTseq-Count) to identify DEGs [14]. The top 20 DEGs were performed by heat map.

2.3. Functional enrichment analysis

DEGs with the threshold for $|\log_{2}FC| > 1.5$ and $\text{padj} < 0.05$ were applied for functional enrichment analysis. Gene Ontology (GO) functional analysis comprising cellular component (CC), molecular function (MF), and biological process (BP), as well as Kyoto Encyclopedia of Genes and Genomes (KEGG) pathway analysis, were implemented using the ClusteProfiler package in R [15].

2.4. Gene set enrichment analysis (GSEA)

R package ClusteProfiler (3.14.3) was used for GSEA to elucidate the functional and pathway differences between the high- and low-expression groups of VTA1. The gene set was permuted 1,000 times for each analysis. Adjusted P-value < 0.05 and FDR q-value < 0.25 were considered to be statistically significant.

2.5. Immune infiltration analysis by single-sample Gene Set Enrichment Analysis (ssGSEA)

Immune infiltration analysis of VTA1 was conducted by ssGSEA using GSVA package in R (3.6.3). A total of 24 types of infiltrating immune cells were obtained as previously described [16]. Spearman correction was used to analyze the correlation between VTA1 and the enrichment scores of 24 types of immune cells. Wilcoxon rank-sum test was used to analyze the enrichment scores of high- and low-VTA1 expression groups.

2.6. PPI network

The PPI network of DEGs was predicted using the Search Tool for the Retrieval of Interacting Genes (STRING) database [17]. The interaction score threshold of 0.4 was set as the cut-off criterion. The PPI network was mapped using Cytoscape (version 3.7.1) [18], and the most significant modules in the PPI network were identified using MCODE (version 1.6.1) [19]. Selection criteria were as follows: MCODE scores > 5 , degree cut-off = 2, node score cut-off = 0.2, Max depth = 100, and k-score = 2. Metascape (<https://metascape.org/gp/index.htm>) was used to conduct the pathway and process enrichment analysis.

2.7. Prognostic model generation and prediction

In order to individualize the prediction of overall survival (OS) and event-free survival (EFS) in LUAD patients, a nomogram was generated using the RMS R package (version 5.1-3), which included prominent clinical characteristics and calibration plots. The calibration curves were evaluated graphically by mapping the nomogram-predicted probabilities against the observed rates, and the 45° line represented the best predictive values. The concordance index (C-index) was used to determine the discrimination of the nomogram, and the bootstrap approach was used to calculate 1000 resamples. In addition, C-index and receiver operating characteristic (ROC) were used to analyze and compare the predictive accuracy of the nomogram and separate prognostic factors. All statistical tests were double-tailed with 0.05 as the statistical significance level.

2.8. Statistical analysis

All statistical analyses and graphs were analyzed and displayed by R (3.6.2) [20]. The expression of VTA1 in unpaired samples was analyzed by the Wilcoxon rank-sum test, with the Wilcoxon signed-rank test used in paired samples. Kruskal-Wallis test, Wilcoxon signed-rank test, and logistic regression analysis were used to evaluate the relationship between clinical/cytogenetic characteristics and VTA1 expression. Cox regression analysis and Kaplan-Meier method were used to evaluate the prognostic factors. Multivariate Cox analysis was adopted to compare the impact of VTA1 expression on survival along with other clinical features. The median VTA1 expression was regarded as the cut-off value. In all tests, P value < 0.05 was considered statistically significant. Moreover, ROC analysis was performed on the pROC package to assess the effectiveness of the transcriptional expression of VTA1 in distinguishing LUAD from healthy samples. The computed area under the curve (AUC) value ranging from 0.5 to 1.0 indicated 50-100% discrimination ability.

3. Results

3.1. VTA1 expression in pan-cancers and LUAD

RNA-seq data from UCSC XENA (<https://xenabrowser.net/datapages/>) was downloaded in TCGA and GTEx formats and processed uniformly through the toiling process. By comparing the expression of VTA1 normal samples in TCGA and GTEx databases and corresponding tumor samples in the TCGA database, VTA1 was found significantly highly expressed in 26 types of cancer (Figure 1A), including lung adenocarcinoma (LUAD) (Figure 1B).

3.2. Identification of DEGs in LUAD samples with low- and high-expressed VTA1

The high- and low-expression groups' gene expression profiles were analyzed for differences in the median mRNA expression. A total of 4968 DEGs from gene expression RNA-seq-HTSeq-Counts, including 736 up-regulated and 4232 down-regulated, were identified as statistically significant between VTA1 high- and low-expressed groups ($|\log \text{fold change} (\log \text{FC})| > 1.5$, $P < 0.05$) (Figure 2A). The top ten up-regulated DEGs and top ten down-regulated DEGs between VTA1 high- and low-expressed groups were illustrated by the heat map (Figure 2B).

3.3. Functional enrichment analysis of DEGs

To better understand the functional implication of 4968 DEGs between high- and low-expression of VTA1 in LUAD, GO and KEGG functional enrichment analysis was performed by clusterProfiler package (Figure 3). The association with the biological process (BP) included pattern specification process, regionalization, and mesenchyme development; cellular components (CC) included

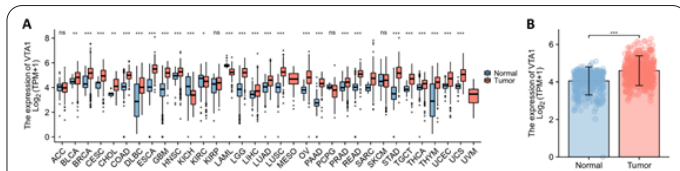


Fig. 1. The higher expression of VTA1 was shown in LUAD compared with normal samples. (A) Expression level of VTA1 in paired normal and pan-cancer samples. (B) Expression level of VTA1 in paired normal and LUAD samples. Analysis between two groups: Wilcoxon Rank sum test; NS: $P \geq 0.05$ or higher; * $P < 0.05$; ** $P < 0.01$; *** $P < 0.001$.

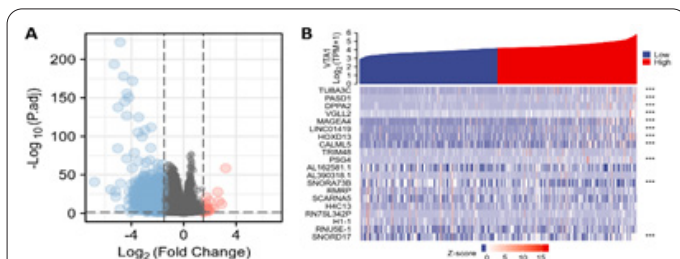


Fig. 2. A total of 4968 DEGs were identified as being statistically significant between VTA1 high-expressed and low-expressed groups. (A) Volcano plot of differentially expressed genes, including 736 up-regulated and 4232 down-regulated genes. Normalized expression levels were shown in descending order from green to red. (B) Heat map of the 20 differentially expressed RNAs, including 10 up-regulated genes and 10 down-regulated genes. The X-axis represents the samples, while the Y-axis denotes the differentially expressed RNAs. Green and red tones represented down-regulated and up-regulated genes, respectively.

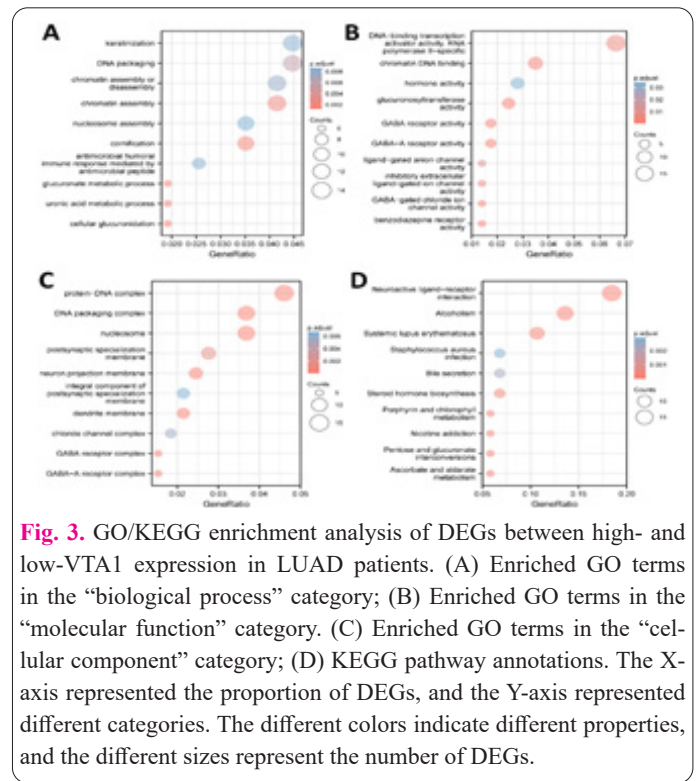


Fig. 3. GO/KEGG enrichment analysis of DEGs between high- and low-VTA1 expression in LUAD patients. (A) Enriched GO terms in the “biological process” category; (B) Enriched GO terms in the “molecular function” category. (C) Enriched GO terms in the “cellular component” category; (D) KEGG pathway annotations. The X-axis represented the proportion of DEGs, and the Y-axis represented different categories. The different colors indicate different properties, and the different sizes represent the number of DEGs.

collagen-containing extracellular matrix, ion channel complex, and basement membrane; molecular function (MF) included receptor ligand activity, DNA-binding transcription activator activity/RNA polymerase II-specific, extracellular matrix structural constituent. KEGG included PI3K-Akt signaling pathway, focal adhesion, and ECM-receptor interaction.

GSEA analysis was conducted to gain further insight into the biological pathways involved in LUAD with different VTA1 expression levels. GSEA was performed between low- and high-VTA1 expression datasets to identify critical signaling pathways involved in LUAD. Significant differences ($FDR < 0.05$, $ADJ P < 0.05$) were observed in the enrichment of MSigDB Collection (C2.all.v7.0.symbols.gmt) of these pathways (Figure 4). Factors with a good prognosis of LUAD, such as neuronal system, HDACs deacetylate histones, HCMV late events, DNA methylation, and pre-notch expression and processing, were enriched in VTA1 low-expression phenotype based on NES, with adjusted P value < 0.05 and FDR value < 0.05 (Figure 4A–4E). On the contrary, in the high expression of VTA1 phenotypes, factors with poor prognosis in LUAD, such as transcriptional regulation by TP53, neuroactive ligand-receptor interaction, mitotic metaphase and anaphase, and biological oxidations, presented significantly enriched (Figure 4F–4I).

3.4. Immune infiltration analysis in LUAD

Spearman correlation analysis showed that the expression level of VTA1 in the LUAD microenvironment was correlated with the immune cell infiltration level quantified by SSGSEA. Specifically, VTA1 was positively associated with Th2 cells and T helper cells (Figure 5).

3.5. PPI enrichment analysis in LUAD

The network of VTA1 and its potential coexpressed genes in VTA1-related DEGs was constructed by STRING, with a threshold of 0.4. A total of 4968 DEGs were screened out ($|\log \text{fold change} (\log \text{FC})| > 1.5$, $P <$

0.05). The PPI network with 36 nodes and 217 edges was displayed by Cytoscape-MCODE (Figure 6A). The most significant module with an MCODE score of 7.317 contained 11 nodes and 55 edges (Figure 6B). Meantime, Metascape-MCODE was used to identify densely connected PPI network components of VTA1.

3.6. Association between VTA1 expression and clinical features and cytogenetic risks

The main clinical characteristics of LUAD in TCGA are shown in Table 1. A total of 535 cases (286 females and 249 males) were analyzed in this study, with an average age of 66.0 years. Among them, VTA1 expression was low in 267 (49.9%) LUAD patients and high in the remaining 268 (50.1%) cases. The median VTA1 expression ($\log_2(\text{TPM}+1)$), which is 5.783, was regarded as the cut-off value. Correlation analysis suggested that VTA1

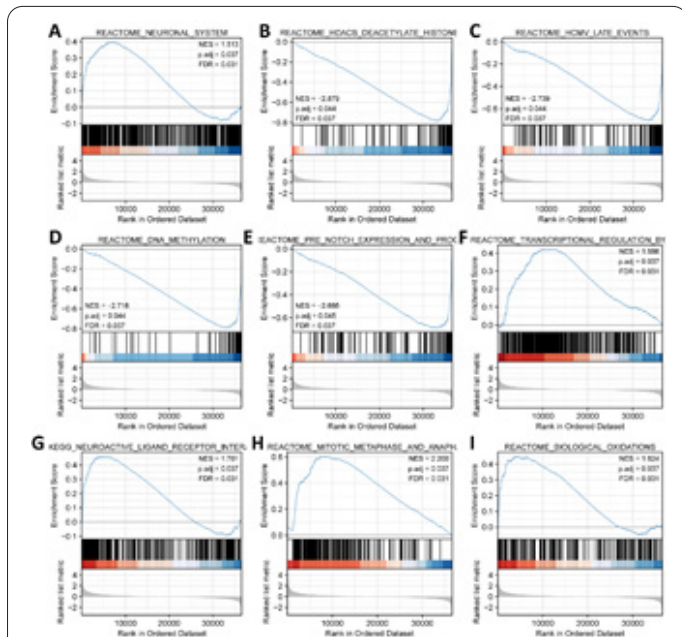


Fig. 4. Enrichment plots from the gene set enrichment analysis (GSEA). (A–I) ES, enrichment score; NES, normalized ES; ADJ P-val, adjusted P-value.

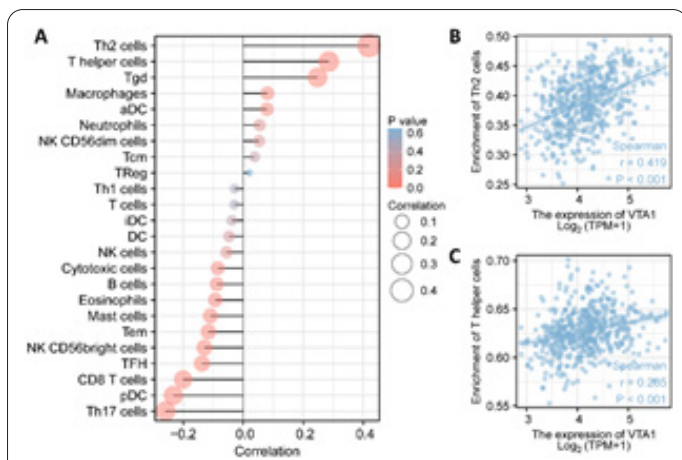


Fig. 5. The expression of VTA1 was associated with immune infiltration in the LUAD microenvironment. (A), The forest plots showed a positive correlation between VTA1 and 9 immune cells and a negative correlation between VTA1 and 15 immune cell subsets. The size of the dots showed the absolute value of Spearman r. (B) Correlation between the relative enrichment score of Th2 cells and the expression level (TPM) of VTA1. (C) Correlation between the relative enrichment score of T helper cells and the expression level (TPM) of VTA1.

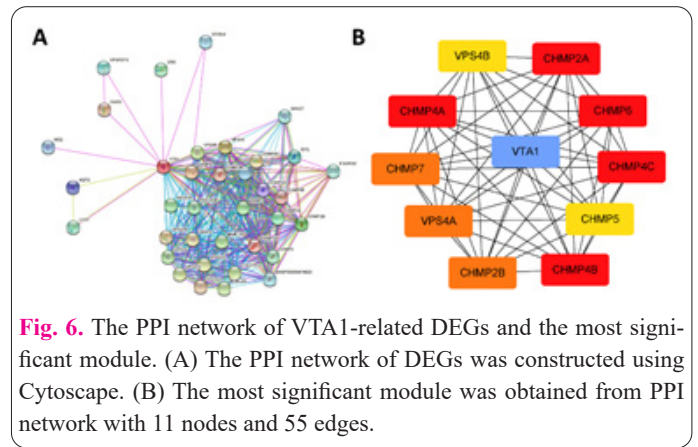


Fig. 6. The PPI network of VTA1-related DEGs and the most significant module. (A) The PPI network of DEGs was constructed using Cytoscape. (B) The most significant module was obtained from PPI network with 11 nodes and 55 edges.

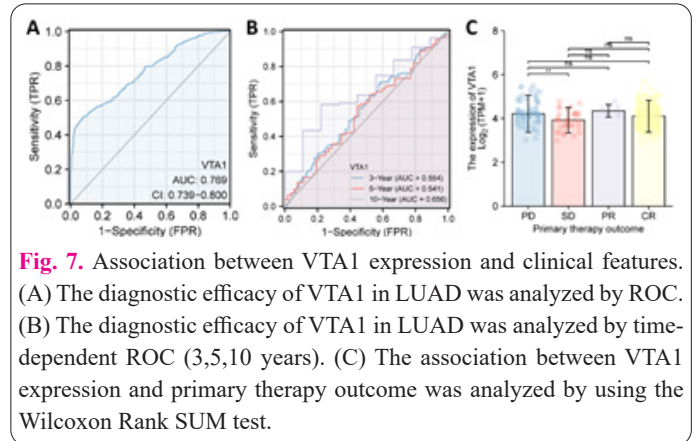


Fig. 7. Association between VTA1 expression and clinical features. (A) The diagnostic efficacy of VTA1 in LUAD was analyzed by ROC. (B) The diagnostic efficacy of VTA1 in LUAD was analyzed by time-dependent ROC (3,5,10 years). (C) The association between VTA1 expression and primary therapy outcome was analyzed by using the Wilcoxon Rank SUM test.

expression was significantly correlated with different T stages ($P < 0.05$). In addition, VTA1 expression was significantly associated with other factors including primary therapy outcome, N stage, M stage, pathologic stage, and residual tumor stage.

Logistic analysis was applied to further verify the relationship between LUAD clinicopathological factors and the VTA1 high-low dichotomy. As a result, high expression of VTA1 showed a significant positive correlation with different T stage (odds ratio, 1.482; $P < 0.05$) (Table 2). What is more, the potential value of VTA1 in differentiating LUAD patients from healthy individuals was examined by ROC curve analysis, with an AUC of 0.769, revealing that VTA1 had potential as a biomarker (Figure 7A). Besides, the potential value of VTA1 in differentiating LUAD patients from healthy individuals was examined by time-dependent ROC curves (3,5,10 years) analysis, with AUCs of 0.554, 0.541, and 0.656, respectively, indicating the potential of VTA1 as a biomarker (Figure 7B). Meanwhile, the Wilcoxon Rank SUM test was used to compare the expression of VTA1 in patients with different efficacy evaluation criteria. The results showed that VTA1 was significantly overexpressed in patients with PD (progressive disease) cancer efficacy (Figure 7C).

3.7. High VTA1 impacted the prognosis of LUAD in patients with different clinicopathological status

The relationship between VTA1 expression and prognosis was analyzed in LUAD patients by using Kaplan-Meier. As seen in Figure 8A, patients with high expression of VTA1 had a significantly worse prognosis than those with low VTA1 expression (hazard ratio (HR), 1.36 (1.02-1.81); $P = 0.036$). Kaplan-Meier analysis presented that high expressed VTA1 correlated with poor prognosis in the subgroups of female gender ($P = 0.049$), and age over

Table 1. Association between VTA1 expression and clinicopathologic features in LUAD samples from the TCGA database.

Characteristic	Low expression of VTA1	High expression of VTA1	P
n	267	268	
T stage, n (%)			0.095
T1	99 (18.6%)	76 (14.3%)	
T2	138 (25.9%)	151 (28.4%)	
T3	23 (4.3%)	26 (4.9%)	
T4	6 (1.1%)	13 (2.4%)	
N stage, n (%)			0.668
N0	179 (34.5%)	169 (32.6%)	
N1	48 (9.2%)	47 (9.1%)	
N2	32 (6.2%)	42 (8.1%)	
N3	1 (0.2%)	1 (0.2%)	
M stage, n (%)			0.650
M0	169 (43.8%)	192 (49.7%)	
M1	10 (2.6%)	15 (3.9%)	
Pathologic stage, n (%)			0.327
Stage I	156 (29.6%)	138 (26.2%)	
Stage II	59 (11.2%)	64 (12.1%)	
Stage III	38 (7.2%)	46 (8.7%)	
Stage IV	10 (1.9%)	16 (3%)	
Primary therapy outcome, n (%)			0.037
PD	30 (6.7%)	41 (9.2%)	
SD	24 (5.4%)	13 (2.9%)	
PR	1 (0.2%)	5 (1.1%)	
CR	178 (39.9%)	154 (34.5%)	
Gender, n (%)			0.317
Female	149 (27.9%)	137 (25.6%)	
Male	118 (22.1%)	131 (24.5%)	
Race, n (%)			0.298
Asian	4 (0.9%)	3 (0.6%)	
Black or African American	34 (7.3%)	21 (4.5%)	
White	206 (44%)	200 (42.7%)	
Age, n (%)			0.662
<=65	126 (24.4%)	129 (25%)	
>65	135 (26.2%)	126 (24.4%)	
Residual tumor, n (%)			0.146
R0	182 (48.9%)	173 (46.5%)	
R1	6 (1.6%)	7 (1.9%)	
R2	0 (0%)	4 (1.1%)	
Anatomic neoplasm subdivision, n (%)			0.539
Left	97 (18.7%)	108 (20.8%)	
Right	159 (30.6%)	156 (30%)	
Anatomic neoplasm subdivision2, n (%)			0.354
Central Lung	34 (18%)	28 (14.8%)	
Peripheral Lung	59 (31.2%)	68 (36%)	
number_pack_years_smoked, n (%)			0.443
<40	102 (27.6%)	86 (23.3%)	
>=40	90 (24.4%)	91 (24.7%)	
Smoker, n (%)			0.327
No	33 (6.3%)	42 (8.1%)	
Yes	227 (43.6%)	219 (42%)	
OS event, n (%)			0.134
Alive	180 (33.6%)	163 (30.5%)	
Dead	87 (16.3%)	105 (19.6%)	

DSS event, n (%)			0.242
Alive	199 (39.9%)	180 (36.1%)	
Dead	55 (11%)	65 (13%)	
PFI event, n (%)			0.565
Alive	158 (29.5%)	151 (28.2%)	
Dead	109 (20.4%)	117 (21.9%)	
Age, median (IQR)	67 (59, 72)	65 (59, 72)	0.992

Table 2. The relationship between the clinicopathological factors of LUAD and VTA1 expression by using logistic analysis.

Characteristics	Total(N)	Odds Ratio (OR)	P value
T stage (T2&T3&T4 vs. T1)	532	1.482 (1.031-2.137)	0.034
N stage (N1&N2&N3 vs. N0)	519	1.177 (0.816-1.699)	0.384
M stage (M1 vs. M0)	386	1.320 (0.584-3.110)	0.510
Pathologic stage (Stage II&Stage III&Stage IV vs. Stage I)	527	1.331 (0.943-1.881)	0.104
Primary therapy outcome (SD&PR&CR vs. PD)	446	0.620 (0.369-1.032)	0.068
Gender (Male vs. Female)	535	1.207 (0.859-1.698)	0.277
Race (White vs. Asian&Black or African American)	468	1.537 (0.895-2.685)	0.123
Age (>65 vs. <=65)	516	0.912 (0.645-1.288)	0.599
Residual tumor (R1&R2 vs. R0)	372	1.929 (0.718-5.704)	0.205
Anatomic neoplasm subdivision (Right vs. Left)	520	0.881 (0.619-1.253)	0.481
Anatomic neoplasm subdivision2 (Peripheral Lung vs. Central Lung)	189	1.400 (0.762-2.588)	0.280
number_pack_years_smoked (>=40 vs. <40)	369	1.199 (0.797-1.807)	0.384
Smoker (Yes vs. No)	521	0.758 (0.461-1.238)	0.270

65 (P = 0.003) (Figure 8B, 8C).

Likewise, the forest plot illustrated the prognostic value of VTA1 in various LUAD subtypes using univariate Cox regression, with a conclusion consistent with the above results (Figure 9).

Hereafter, univariate Cox proportional hazards regression was used to assess the factors influencing OS, disclosing that VTA1 (high- vs. low-, P = 0.036) was a predictive factor for worse OS, so did T stage (T2&T3&T4 vs. T1, P < 0.05), N stage (N1&N2&N3 vs. N0, P < 0.001), M stage (M1 vs. M0, P < 0.01), pathologic stage (stage II&III&IV vs. stage I, P < 0.001), and residual tumor stage (R1&R2 vs. R0, P < 0.001) (Table 3). T stage, N stage, M stage, pathologic stage, primary therapy outcome, residual tumor stage and VTA1 were then included in multivariate Cox regression, suggesting that T3 (P = 0.022), N1 (P = 0.044), and CR (P = 0.013) were independent prognostic factors for worse OS (P < 0.05).

3.8. Prognostic model of VTA1 in LUAD

To better predict LUAD patients' prognosis, a nomogram was constructed based on the Cox regression analysis

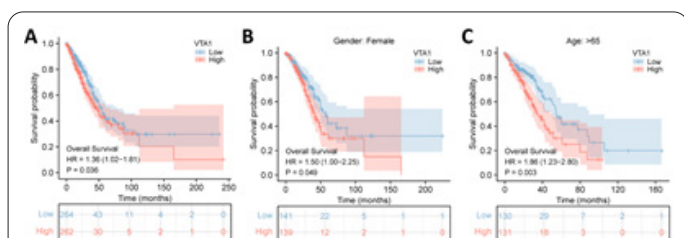


Fig. 8. Association between VTA1 expression and clinical features. (A) The diagnostic efficacy of VTA1 in LUAD was analyzed by ROC. (B) The diagnostic efficacy of VTA1 in LUAD was analyzed by time-dependent ROC (3,5,10 years). (C) The association between VTA1 expression and primary therapy outcome was analyzed by using the Wilcoxon Rank SUM test.

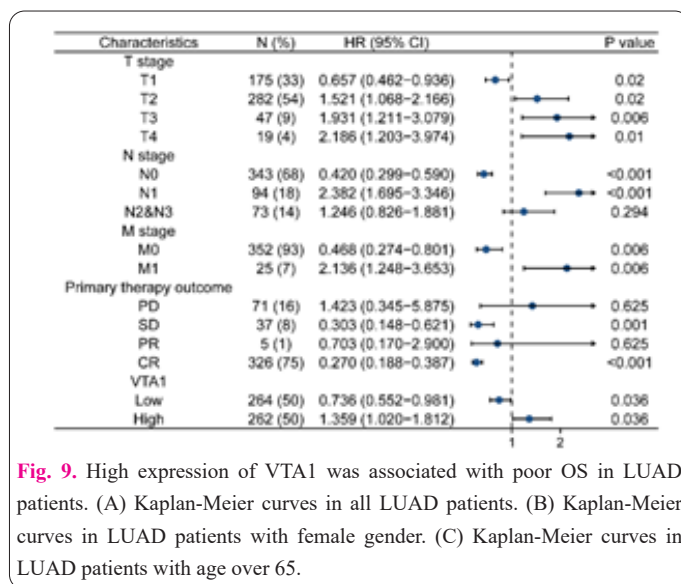


Fig. 9. High expression of VTA1 was associated with poor OS in LUAD patients. (A) Kaplan-Meier curves in all LUAD patients. (B) Kaplan-Meier curves in LUAD patients with female gender. (C) Kaplan-Meier curves in LUAD patients with age over 65.

results using the RMS R package (Figure 10A). Four independent prognostic factor variables, T stage, N stage, primary therapy outcome, and VTA1 expression, were included in the model and selected into the prediction model at a statistical significance level of 0.2. Based on multivariate Cox analysis, a point scale was used to assign points to these variables. The straight line was drawn upward to determine the points of the variables, and the sum of the points assigned to each variable was rescaled to a range of 0–100. The points of each variable were accumulated and recorded as the total points. The probability of LUAD patient survival at 1-, 5-, and 10 years was determined by drawing a line from the total point axis straight down to the outcome axis. The 1-year survival probability was determined by drawing a vertical line downward on the total point axis along the 162-direction ending axis, suggesting the probability of 1-year survival < 40%, both of the probability of 5- and 10-year < 10%. The prediction results

Table 3. Univariate and multivariate Cox's regression analysis of factors associated with OS in LUAD.

Characteristics	Total(N)	Univariate analysis		Multivariate analysis	
		Hazard ratio (95% CI)	P value	Hazard ratio (95% CI)	P value
T stage	523				
T1	175	Reference			
T2	282	1.521 (1.068-2.166)	0.020	1.141 (0.656-1.984)	0.641
T3	47	2.937 (1.746-4.941)	<0.001	3.432 (1.196-9.850)	0.022
T4	19	3.326 (1.751-6.316)	<0.001	2.241 (0.685-7.335)	0.182
N stage	510				
N0	343	Reference			
N1	94	2.382 (1.695-3.346)	<0.001	2.854 (1.029-7.916)	0.044
N2&N3	73	2.968 (2.040-4.318)	<0.001	3.055 (0.912-10.237)	0.070
M stage	377				
M0	352	Reference			
M1	25	2.136 (1.248-3.653)	0.006	1.238 (0.386-3.969)	0.720
Pathologic stage	518				
Stage I	290	Reference			
Stage II	121	2.418 (1.691-3.457)	<0.001	0.525 (0.183-1.506)	0.231
Stage III	81	3.544 (2.437-5.154)	<0.001	0.800 (0.205-3.128)	0.749
Stage IV	26	3.790 (2.193-6.548)	<0.001		
Primary therapy outcome	439				
PR	5	Reference			
SD	37	0.432 (0.093-2.005)	0.284	0.236 (0.042-1.323)	0.101
PD	71	1.423 (0.345-5.875)	0.625	0.683 (0.152-3.076)	0.620
CR	326	0.384 (0.094-1.566)	0.182	0.157 (0.036-0.675)	0.013
Gender	526				
Female	280	Reference			
Male	246	1.070 (0.803-1.426)	0.642		
Race	468				
Asian	7	Reference			
Black or African American	55	1.408 (0.187-10.599)	0.740		
White	406	2.030 (0.284-14.519)	0.481		
Age	516				
<=65	255	Reference			
>65	261	1.223 (0.916-1.635)	0.172		
Residual tumor	363				
R0	347	Reference			
R1	13	3.255 (1.694-6.251)	<0.001	2.683 (0.938-7.678)	0.066
R2	3	11.085 (3.443-35.689)	<0.001		
Anatomic neoplasm subdivision	512				
Left	200	Reference			
Right	312	1.037 (0.770-1.397)	0.810		
Anatomic neoplasm subdivision2	182				
Central Lung	62	Reference			
Peripheral Lung	120	0.913 (0.570-1.463)	0.706		
number_pack_years_smoked	363				
<40	183	Reference			
>=40	180	1.073 (0.753-1.528)	0.697		
Smoker	512				
No	72	Reference			
Yes	440	0.894 (0.592-1.348)	0.591		
VTA1	526				
Low	264	Reference			
High	262	1.359 (1.020-1.812)	0.036	1.195 (0.763-1.870)	0.436

of the nomogram calibration curve of OS were consistent with all patients' observation results (Figure 10B).

4. Discussion

Vesicle Trafficking 1 (VTA1) is a gene that codes for proteins. Both Arthrogyrosis, Distal, Type 1B and Arthrogyrosis, Distal, Type 1A are diseases connected to VTA1. The HIV Life Cycle and vesicle-mediated transport are two of its linked mechanisms. In solid human tumors, VTA1 has been linked to tumor progression. VTA1 participates in the multivesicular body's functions, which include sorting membrane proteins for lysosomal breakdown. VPS4A/B is hypothesized to have VTA1 as a cofactor. HIV-1 budding is aided by VTA1. Similarity has demonstrated that it plays a role in the classification and down-regulation of EGFR [21,22]. The endosomal multivesicular bodies (MVB) route involves VTA1. Intraluminal vesicles (ILVs) produced by invagination and scission from the endosome's limiting membrane are seen in MVBs. These ILVs are mostly transported to lysosomes where they enable the destruction of membrane proteins such as activated growth factor receptors, lysosomal enzymes, and lipids. VPS4A/B, which catalyzes the disassembly of membrane-associated ESCRT-III assemblies, is considered to work with VTA1 as a cofactor. By similarities, VTA1 is also implicated in EGFR sorting and down-regulation. The expression of VTA1 in LUAD and its prognostic significance, however, are yet unknown [23,24].

The present study's central result was that high-expressed VTA1 in LUAD was associated with different pathological stages of cancer and poor prognosis. Via GSEA gene enrichment analysis, low-expressed VTA1 was associated with neuronal system, HDACs deacetylate histones, HCMV late events, DNA methylation, and pre-notch expression and processing, which are excellent prognostic factors. In contrast, high-expressed VTA1 was associated with transcriptional regulation by TP53, neuroactive ligand-receptor interaction, mitotic metaphase and anaphase, and biological oxidations, suggesting that VTA1 was not only a potential prognostic biomarker but also a promising therapeutic target by affecting oncogenesis-related pathways in LUAD [25,26].

It is worth noting that the most clinically relevant finding was that high expression of VTA1 was associated with poor survival. Multivariate Cox regression analysis showed that high expression of VTA1 was independent prognostic factor with T stage T3, N stage N1, and primary therapy outcome CR. The establishment of the nomogram prediction model further confirmed the predictive effect of VTA1 expression on prognosis. Therefore, VTA1 may serve as a new adverse prognostic factor in LUAD patients [27].

In immune cell infiltration analysis, high expression of VTA1 was associated with Th2 cells and T helper cells. Due to the ability of both Th1 and Th2 cells to secrete cytokines to promote their proliferation and inhibit the proliferation of the other, Th1 and Th2 cells are in a relatively balanced state in the body under normal circumstances. But when the body experiences functional abnormalities, it often shows a balance deviation towards one side, known as "Th1/Th2 drift". Once the balance between Th1 cells and Th2 cells is broken, it is likely to cause the dynamic balance of human cytokine network to be broken, thus causing the emergence and development of many diseases.

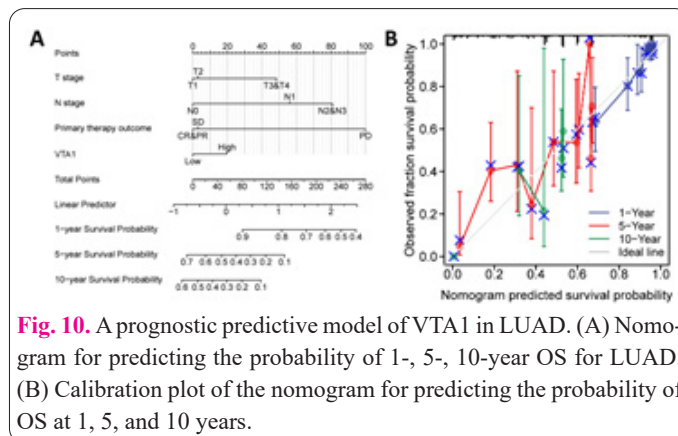


Fig. 10. A prognostic predictive model of VTA1 in LUAD. (A) Nomogram for predicting the probability of 1-, 5-, 10-year OS for LUAD. (B) Calibration plot of the nomogram for predicting the probability of OS at 1, 5, and 10 years.

Th1/Th2 balance drift exists in many tumors, including lung cancer, glioma, cervical cancer, breast cancer, gastric cancer, colorectal cancer and other patients. Th2 cells are often dominant, which may be related to tumor immune escape. In this study, Th2 and T helper cells' infiltration was positively correlated with VTA1 expression. Through Kaplan-Meier survival analysis, high VTA1 expression was found to be associated with poor prognosis in LUAD patients. LUAD blast cells have been reported to evade Th2 cell immunosurveillance by diminishing the expression of several activated receptors. However, the relationship between Th2 and T helper cells with LUAD has not been fully elaborated. Hence, according to our findings and the above research reports, the relationship between VTA1 with Th2 and T helper cells, and whether VTA1 and Th2 and T helper cells are involved in the immune escape in LUAD still deserve further exploration [28,29].

Moreover, Cox analysis in the present study indicated that VTA1 might have the ability to become an independent predictor of poor prognosis in LUAD after adjusting for routine clinical features. Multivariate Cox regression analysis showed that T stage T3, N stage N1, primary therapy outcome CR and high VTA1 expression were the independent prognostic factors for OS deterioration. A nomogram prognosis map was constructed by combining VTA1 with T stage, N stage and primary therapy outcome to obtain a more accurate prognosis prediction model. The C-index VTA1-related Cox model predicted the OS to be 0.769 (0.739–0.800). The calibration chart showed optimal agreement between the predictions of the nomogram associated with VTA1 and the actual observations of 1-year, 5-year, and 10-year OS probabilities. As previously reported, T stage T2&T3&T4, N stage N1&N2&N3, M stage M1, pathologic stage II&III&IV, primary therapy outcome CR, and residual tumor R1&R2 were independent factors predicting poor prognosis of LUAD. According to the Cox analysis and nomogram model, it seems that VTA1 may potentially have better predictive power than other factors. From this point of view, our model may provide a personalized score for individual LUAD patients [30,31].

However, the limitation of this study lies in the small sample size. Also, to ensure greater reliability and representativeness of the findings and assumptions, the sample should be expanded for further research in the future. Clinical samples should be used to verify the prognostic predictive role of VTA1 mRNA and protein in LUAD. Experimental validation should also be performed to investigate the regulatory mechanisms between VTA1 and the genetic alterations and essential pathways selected by

GSEA analysis. A mass of plans has been formulated for some recent laboratory work.

5. Conclusion

In summary, this study disclosed for the first time that VTA1 expression increased in LUAD, which is also related to poor prognosis. Moreover, transcriptional regulation by TP53, neuroactive ligand-receptor interaction, mitotic metaphase and anaphase, and biological oxidations may be the essential pathways participating in the regulation of VTA1 in LUAD. Further verification should be carried out to reveal the biological impacts of VTA1 in LUAD.

Acknowledgments

We would like to acknowledge everyone for their helpful contributions to this paper.

Competing interests

The authors declared that they have no competing interests.

Consent for publications

The author read and approved the final manuscript for publication.

Ethics approval and consent to participate

The research protocol has been reviewed and approved by the Ethical Committee and Institutional Review Board of the Huzhou Hospital of Traditional Chinese Medicine, Zhejiang University of Traditional Chinese Medicine.

Informed Consent

The authors declare not used any patients in this research.

Availability of data and material

The data that support the findings of this study are available from the corresponding author upon reasonable request

Authors' contributions

Xingang Sun, Ruixin Wu and Xinjun Guan designed the study and performed the experiments, Changsheng Dong, Dongze Qiu and Guojie Xia collected the data, Shouhan Feng, Jinlong Duan and Lei Zhang analyzed the data, Xingang Sun, Ruixin Wu and Xinjun Guan prepared the manuscript. All authors read and approved the final manuscript.

Funding

Foundation of Shanghai Changning District Municipal Commission of Health and Family Planning (Grant No. 20154Y019).

References

- Butnor KJ (2020) Controversies and challenges in the histologic subtyping of lung adenocarcinoma. *Transl Lung Cancer Res* 9:839-846. doi: 10.21037/tlcr.2019.12.30
- Tonyali O, Gonullu O, Ozturk MA, Kosif A, Civi OG (2020) Hepatoid adenocarcinoma of the lung and the review of the literature. *J Oncol Pharm Pract* 26:1505-1510. doi: 10.1177/1078155220903360
- Succony L, Rassl DM, Barker AP, McCaughan FM, Rintoul RC (2021) Adenocarcinoma spectrum lesions of the lung: Detection, pathology and treatment strategies. *Cancer Treat Rev* 99:102237. doi: 10.1016/j.ctrv.2021.102237
- Fanning S, Selkoe D, Dettmer U (2021) Vesicle trafficking and lipid metabolism in synucleinopathy. *Acta Neuropathol* 141:491-510. doi: 10.1007/s00401-020-02177-z
- Kwon C, Lee JH, Yun HS (2020) SNAREs in Plant Biotic and Abiotic Stress Responses. *Mol Cells* 43:501-508. doi: 10.14348/molcells.2020.0007
- Makowski SL, Kuna RS, Field SJ (2020) Induction of membrane curvature by proteins involved in Golgi trafficking. *Adv Biol Regul* 75:100661. doi: 10.1016/j.jbior.2019.100661
- Arrazola SA, Luque MM, Lacerda HM, Llaverro F, Zugaza JL (2021) Small GTPases of the Rab and Arf Families: Key Regulators of Intracellular Trafficking in Neurodegeneration. *Int J Mol Sci* 22:4425. doi: 10.3390/ijms22094425
- Yarwood R, Hellicar J, Woodman PG, Lowe M (2020) Membrane trafficking in health and disease. *Dis Model Mech* 13:dmm043448. doi: 10.1242/dmm.043448
- Hao GJ, Zhao XY, Zhang MM, Ying J, Yu F, Li S et al (2022) Vesicle trafficking in Arabidopsis pollen tubes. *Febs Lett* 596:2231-2242. doi: 10.1002/1873-3468.14343
- Vivian J, Rao AA, Nothaft FA, Ketchum C, Armstrong J, Novak A et al (2017) Toil enables reproducible, open source, big biomedical data analyses. *Nat Biotechnol* 35:314-316. doi: 10.1038/nbt.3772
- Goldman MJ, Craft B, Hastie M, Repecka K, McDade F, Kamath A et al (2020) Visualizing and interpreting cancer genomics data via the Xena platform. *Nat Biotechnol* 38:675-678. doi: 10.1038/s41587-020-0546-8
- Li K, Luo H, Luo H, Zhu X (2020) Clinical and prognostic pan-cancer analysis of m6A RNA methylation regulators in four types of endocrine system tumors. *Aging (Albany Ny)* 12:23931-23944. doi: 10.18632/aging.104064
- Thimmareddygar D, Ramahi A, Chan KH, Patel R, Bellary S, Sharma H et al (2021) An Unusual Presentation of Aggressive Primary Invasive Adenocarcinoma of Lung. *Am J Med Sci* 361:118-125. doi: 10.1016/j.amjms.2020.09.014
- Love MI, Huber W, Anders S (2014) Moderated estimation of fold change and dispersion for RNA-seq data with DESeq2. *Genome Biol* 15:550. doi: 10.1186/s13059-014-0550-8
- Yu G, Wang LG, Han Y, He QY (2012) clusterProfiler: an R package for comparing biological themes among gene clusters. *Omics* 16:284-287. doi: 10.1089/omi.2011.0118
- Bindea G, Mlecnik B, Tosolini M, Kirilovsky A, Waldner M, Obenauf AC et al (2013) Spatiotemporal dynamics of intratumoral immune cells reveal the immune landscape in human cancer. *Immunity* 39:782-795. doi: 10.1016/j.immuni.2013.10.003
- Szklarczyk D, Gable AL, Lyon D, Junge A, Wyder S, Huerta-Cepas J et al (2019) STRING v11: protein-protein association networks with increased coverage, supporting functional discovery in genome-wide experimental datasets. *Nucleic Acids Res* 47:D607-D613. doi: 10.1093/nar/gky1131
- Demchak B, Hull T, Reich M, Liefeld T, Smoot M, Ideker T et al (2014) Cytoscape: the network visualization tool for GenomeSpace workflows. *F1000Res* 3:151. doi: 10.12688/f1000research.4492.2
- Bandettini WP, Kellman P, Mancini C, Booker OJ, Vasu S, Leung SW et al (2012) MultiContrast Delayed Enhancement (MCOE) improves detection of subendocardial myocardial infarction by late gadolinium enhancement cardiovascular magnetic resonance: a clinical validation study. *J Cardiovasc Magn Reson* 14:83. doi: 10.1186/1532-429X-14-83
- Isidro-Sanchez J, Akdemir D, Montilla-Bascon G (2017) Genome-Wide Association Analysis Using R. *Methods Mol Biol* 1536:189-207. doi: 10.1007/978-1-4939-6682-0_14

21. Behzadmehr R, Rezaie-Keikhaie K (2022) Evaluation of Active Pulmonary Tuberculosis Among Women with Diabetes. *Cell Mol Biol* 2:56-63. doi: 10.55705/cmbr.2022.336572.1036
22. Murphy C, Sheehy N (2017) EGF Uptake and Degradation Assay to Determine the Effect of HTLV Regulatory Proteins on the ESCRT-Dependent MVB Pathway. *Methods Mol Biol* 1582:103-108. doi: 10.1007/978-1-4939-6872-5_8
23. Wong LH, Eden ER, Futter CE (2018) Roles for ER: endosome membrane contact sites in ligand-stimulated intraluminal vesicle formation. *Biochem Soc Trans* 46:1055-1062. doi: 10.1042/BST20170432
24. Ali Salman R (2023) Prevalence of women breast cancer. *Cell Mol Biol* 3:185-196. doi: 10.55705/cmbr.2023.384467.1095
25. Jiang F, Liang M, Huang X, Shi W, Wang Y (2021) High expression of PIMREG predicts poor survival outcomes and is correlated with immune infiltrates in lung adenocarcinoma. *Peerj* 9:e11697. doi: 10.7717/peerj.11697
26. Rezaie-Kahkhaie K, Rezaie-Keikhaie K, Rezaie-Kahkhaie L, Saravani K, Kamali A (2021) The relationship between IL23R 1142G / A (Arg381Gln) and GM-CSF 3928 C / T (Ile117Thr) gene polymorphism in Iranian patients with tuberculosis disease. *Cell Mol Biol* 1:113-121. doi: 10.55705/cmbr.2021.356674.1059
27. Jiawei Z, Min M, Yingru X, Xin Z, Danting L, Yafeng L et al (2020) Identification of Key Genes in Lung Adenocarcinoma and Establishment of Prognostic Mode. *Front Mol Biosci* 7:561456. doi: 10.3389/fmolb.2020.561456
28. Spinner CA, Lamsoul I, Metais A, Febrissy C, Moog-Lutz C, Lutz PG (2019) The E3 Ubiquitin Ligase Asb2alpha in T Helper 2 Cells Negatively Regulates Antitumor Immunity in Colorectal Cancer. *Cancer Immunol Res* 7:1332-1344. doi: 10.1158/2326-6066.CIR-18-0562
29. Yin R, Qu L, Wang Z, Tang J, Gu H, Wang X et al (2023) Prognostic and immunological potential of PPM1G in lung adenocarcinoma. *Mol Med Rep* 28:156. doi: 10.3892/mmr.2023.13043
30. Zhang S, Xiao X, Qin X, Xia H (2023) Development and validation of a nomogram for predicting overall survival in patients with stage III-N2 lung adenocarcinoma based on the SEER database. *Transl Cancer Res* 12:2742-2753. doi: 10.21037/tcr-22-2757
31. Li L, Ren T, Liu K, Li ML, Geng YJ, Yang Y et al (2021) Development and Validation of a Prognostic Nomogram Based on the Systemic Immune-Inflammation Index for Resectable Gallbladder Cancer to Predict Survival and Chemotherapy Benefit. *Front Oncol* 11:692647. doi: 10.3389/fonc.2021.692647